Global Change Biology (2007) **13,** 707–721, doi: 10.1111/j.1365-2486.2006.01311.x

Phenology model from surface meteorology does not capture satellite-based greenup estimations

JEREMY I. FISHER*†, ANDREW D. RICHARDSON† and JOHN F. MUSTARD*
*Department of Geological Sciences, Brown University, Providence, RI 02912, USA, †Complex Systems Research Center, University of New Hampshire, Durham, NH 03824, USA

Abstract

Seasonal temperature change in temperate forests is known to trigger the start of spring growth, and both interannual and spatial variations in spring onset have been tied to climatic variability. Satellite dates are increasingly being used in phenology studies, but to date that has been little effort to link remotely sensed phenology to surface climate records. In this research, we use a two-parameter spring warming phenology model to explore the relationship between climate and satellite-based phenology. We employ daily air temperature records between 2000 and 2005 for 171 National Oceanographic and Atmospheric Administration weather stations located throughout New England to construct spring warming models predicting the onset of spring, as defined by the date of half-maximum greenness (D_{50}) in deciduous forests as detected from Moderate Resolution Imaging Spectrometer. The best spring warming model starts accumulating temperatures after March 20th and when average daily temperatures exceed 5 °C. The accumulated heat sums [heating degree day (HDD)] required to reach D_{50} range from 150 to 300 degree days over New England, with the highest requirements to the south and in coastal regions. We test the ability of the spring warming model to predict phenology against a null photoperiod model (average date of onset). The spring warming model offers little improvement on the null model when predicting D_{50}. Differences between the efficacies of the two models are expressed as the 'climate sensitivity ratio' (CSR), which displays coherent spatial patterns. Our results suggest that northern (beech-maple-birch) and central (oak-hickory) hardwood forests respond to climate differently, particularly with disparate requirements for the minimum temperature necessary to begin spring growth (3 and 6 °C, respectively). We conclude that spatial location and species composition are critical factors for predicting the phenological response to climate change: satellite observations cannot be linked directly to temperature variability if species or community compositions are unknown.

Keywords: climate change, climate coupling, green wave, growing degree days, meteorology data, MODIS, northern deciduous forest, phenology, satellite remote sensing, spring warming model

Received 28 June 2006 and accepted 25 September 2006

Introduction

The abiotic environment regulates physiological processes (metabolism, photosynthesis and respiration), growth, and development of terrestrial vegetation across a wide range of time scales, from hours to decades. For example, interannual temperature variability influences phenology (the seasonal occurrence of developmental and life cycle events; Rathcke & Lacey, 1985) of both agricultural crops (e.g. Cesaraccio *et al*., 2004; Chuine *et al*., 2004) and temperate forest tree species (e.g. Richardson *et al*., 2006).

While it is generally accepted that warmer winter and spring temperatures give rise to earlier (or faster) spring growth (Lechowicz, 1984), the underlying ontogenetic mechanism is still not well understood, and a consensus model of spring phenology has not yet emerged

Correspondence: Jeremy Fisher, Institute for the Study of Earth, Oceans, and Space, 461 Morse Hall, University of New Hampshire, 39 College Road, Durham, NH 03824, USA, tel. +1 603 862 1555, fax +1 603 862 0188, e-mail: jifisher@gmail.com

(compare Hanninen, 1995; Chuine, 2000; Schaber & Badeck, 2003). However, the strong link between seasonal temperature variability and phenological changes suggests that long-term, broad-scale observations of phenology could serve as a proxy for global temperature change over time and space (Myneni *et al*., 1997; White *et al*., 1997). Over the last four to five decades, observed trends toward earlier spring development (budburst or flowering) and later autumn senescence have been attributed to recent warming (White *et al*., 1997; Fitter & Fitter, 2002; Peñuelas *et al*., 2002; Schwartz *et al*., 2002; White & Nemani, 2003; Badeck *et al*., 2004; Chuine *et al*., 2004).

Long-term phenological records have been analyzed to probe the underlying relationships between temperature and phenology (Chuine *et al*., 2004), but there are few spatially extensive ground-based field observations, particularly in North America (Schwartz *et al*., 2006). To this end, satellite records of phenology may provide the opportunity to scale ground-based phenological observations and test models of phenology developed from field data. Within individual years, spatial patterns in satellite-based phenology have been tied to temperature gradients (Zhang *et al*., 2004, Fisher *et al*., 2006) and seasonal water availability (Lotsch *et al*., 2005; Bradley *et al*., 2006), interannual variability has been used to infer climate trends (e.g. Myneni *et al*., 1997; Anyamba *et al*., 2002; Potter *et al*., 2003; Goetz *et al*., 2005; Lotsch *et al*., 2005).

In spite of the spatial and temporal richness of satellite data, to date there have been no efforts to parameterize even simple models using remotely sensed phenological time series in conjunction with surface meteorological data. Global satellite data [e.g. the Moderate Resolution Imaging Spectrometer (MODIS)] and a dense network of climate records [e.g. National Oceanographic and Atmospheric Administration (NOAA) National Climate Data Center (NCDC)] overlap across North American forests, thus allowing the analysis of satellite phenology with ground-based models of climate-forced phenology. Our objective here is to combine these two data sources, thereby developing a framework with which we can try to answer a fundamental question: if temperature is related to the start of the growing season, then to what extent is interannual variability observed in satellite records driven by temperature variation?

Climate-phenology models

Linking ground and satellite studies is made difficult by for a variety of reasons, including uncertainty in satellite data, relatively short (<30 years) satellite records, inadequate spatial and temporal resolution of the satellite records, highly heterogeneous forest landscapes, and numerous mixed species within a pixel (Badeck *et al*., 2004). The task is hampered by the wide range of potential climate-phenology models with highly variable explanatory power, even in single species studies (Chuine *et al*., 1998; Schaber, 2002). Many temperate phenology-climate models have been developed from studies of single species, and are typically not tested at multiple locations (but see Schaber, 2002). Despite these drawbacks, a firm link between climate and vegetation variability as detected from satellites will advance both our understanding of phenology and expected ecosystem responses to global climate change.

Conceptually and operationally, the framework for linking satellite-based deciduous dynamics with climatic data could echo procedures from ground-based analyses, providing time series for simple models driven by climate station data. The developed set of phenology-climate models range from the two parameter 'spring warming' model (Hunter & Lechowicz, 1992; Rötzer *et al*., 2004) to complex models that are considered more 'physiologically realistic' but require numerous parameters (e.g. the parallel model and sequential models: Cannell & Smith, 1983; PIM: Schaber, 2002; SeqSar: Chuine *et al*., 2004).

In the spring warming model, canopy development occurs in response to aggregated heat sums, or heating degree days (HDD), measured as the sum of average daily temperature above a base (T_{base}), starting at day of year (DOY) t_0. The HDD at which a specified level of development has occurred (typically leaf emergence or first flower) is the critical forcing temperature (F^*). Thus, given known constant T_{base} and t_0 parameters, interannual variation in phenology might track the date at which F^*, a constant aggregated heat sum, occurs. A natural 'null model' against which to evaluate the predictions of the spring warming model is one in which DOY (or photoperiod) controls spring onset (e.g. the 'null model' of Chuine, 2000 or Richardson *et al*., 2006). While the spring-warming model predicts different leaf out scenarios in each year depending on interannual temperature variability, the null model predicts no interannual variation (i.e. by definition, vegetation which responds only to day length will always emerge on the same day of the year).

Here, we use 6 years of spatially extensive, but temporally limited (2000–2005), satellite data to parameterize a simple spring warming model, which we choose for two reasons: (1) in a number of studies, the simple spring warming model has been shown to be as accurate as more complex models for predicting the start of spring growth (Chuine *et al*., 1998; Schaber, 2002); and (2) given the short time series and inherently noisy satellite data, there is a high likelihood of overfitting a complex model.

Satellite phenology model

Satellite phenologies are based on two assumptions: first, that canopy greenness as observed from the satellite is related directly to canopy development; second, that discrete time-series measurements represent a continuous function of canopy closure. Previous studies have demonstrated moderate to good agreement between satellite measures of greenness and field-based observations of development (e.g. Jenkins *et al*., 2002; Schwartz *et al*., 2002; Fisher & Mustard, 2006). Here, as previously (Fisher & Mustard, 2006), we use a simple logistic growth (sigmoid) curve to describe the seasonal patterns in greenness while reducing cloud and satellite noise (see also Zhang *et al*., 2003; Beck *et al*., 2005). The specification of an objective criterion for identifying the start of the growing season from the chosen continuous time series is under debate (e.g. differences between Jenkins *et al*., 2002; Zhang *et al*., 2003; Bradley *et al*., 2006; Fisher & Mustard, 2006). In this study, we use the half-maximum greenness ('onset') as a stable marker during greenup (see Fisher & Mustard, 2006, for details).

Judging climate-phenology model efficacy

A significant unresolved failure of many climate-phenology models is their inability to predict spatial variance; while models can predict the interannual variation in phenology at a specific site, a model developed at one site will often fail when applied at another location (Schaber, 2002; Richardson *et al*., 2006). Multiple years of satellite data give us a unique opportunity to test models through two dimensions: across space and time (years, interannually).

We formulate a series of alternative hypotheses, which may be evaluated with remotely sensed phenology data coupled to ground-based climate data.

A. Greenup (the start of the growing season in a forest canopy) is governed by photoperiod, such that the timing of growth is consistent by DOY rather than temperature variability (a.k.a the null model).
B. Greenup is governed by uniform seasonal heat sums (HDD) in a spring warming model such that the timing of growth is predicted by the date at which HDD reaches a consistent F^* value at all locations (Rötzer *et al*., 2004; Cook *et al*., 2005).
C. Greenup is governed by nonuniform HDD in a spring warming model where F^* values vary across space (sites or stations), but are consistent at any given location (Karlsson *et al*., 2003); sites may differ by species, genotype, age, and/or altitude, latitude, and distance from water bodies (Scheifinger *et al*., 2002).
D. Greenup is governed by a combination of HDD and DOY, such that some forests have consistent F^* values, while others become green with uniform DOY; sites may differ by forest composition or location (e.g. drivers are spatially heterogeneous).

Using 6 years of MODIS satellite data (2000–2005) in New England, northeastern United States, we investigate if there is a regionally coherent response to phenological climate forcing. Specifically, we examine whether the null or spring warming model better explains patterns of spring phenology across time and space. We use these results to assess the hypotheses stated above.

Methods

Data preparation

The study region covers southern New England, USA, extending from 40–44°N to 69–76°W (Fig. 1). Lake Ontario, central Maine, and eastern Pennsylvania bound the NW, NE and SW, respectively. This region covers topographic gradients from sea level to over 1400 m, five mountain ranges, and four major land cover types: deciduous and coniferous forests, agricultural lands, and urban areas. Our analysis is based on satellite and weather data for the years 2000–2005.

Daily weather data for 231 NOAA stations within the study region were obtained from the United States National NCDC (http://www.ncdc.noaa.gov/). Average daily temperature was calculated as the mean of the daily maximum (T_{max}) and minimum (T_{min}). We use only data between DOY 1 and 200; stations with more than 5% missing observations between these dates for a given year were not included in the analysis. Data gaps were filled by interpolating temperature from other stations on the basis of elevation and latitude. Stations with fewer than 5 out of 6 years of data were culled, leaving a total of 171 stations in the analysis (Fig. 2).

MODIS bidirectional reflectance corrected spectral data (MOD09A1) were collected over SIN tile h12 v04 between 2/26/2000 and 10/16/2005 from NASA Distributed Active Archive Centers (DAAC, http://nasadaacs.eos.nasa.gov/). We chose seven spectral band data at 500 m spatial resolution (0.25 km^2 $pixel^{-1}$) from 8-day maximum-quality composite data to gather highest information content at the finest feasible temporal and spatial scale. Stations were geolocated in the MODIS data, and reflectance data extracted in a 7×7 grid (3.5 km per side, or 12.25 km^2) centered at the station coordinates. Within each extracted pixel, each seven-band data point (i, represents the ith time incre-

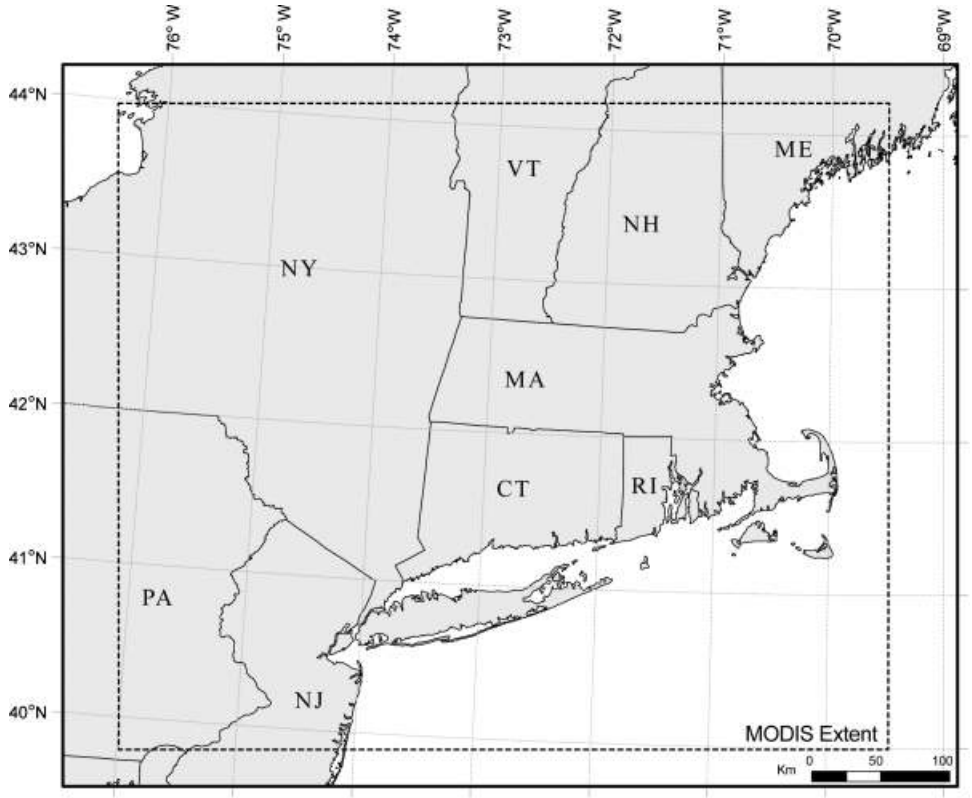

Fig. 1 Spatial extent of Moderate Resolution Imaging Spectrometer image in New England, northeastern USA.

ment in the time series) was unmixed with a linear spectral mixture analysis (SMA, e.g. Adams *et al*., 1993) to derive green vegetation fractional aerial abundance (GV_i at the ith data point) and the residual spectral error ($RMSE_i$). Each GV_i data point was assigned a weight ($w_i = RMSE_i^{-1}$) and a DOY (DOY_i) acquisition date. The DOY_i was obtained from a MODIS metadata layer which specifies the actual overpass day within the composite period (for greater detail on this method, see Fisher & Mustard, 2006). HDD_i were calculated for each data point (i) according to the HDD obtained at DOY_i.

Climate stations in the study region from the NCDC are placed in a variety of different settings, including airports, urban areas, along shorelines, and in agricultural fields or adjacent to forests. Because pixels observed around each station will often not represent contiguous deciduous forest, the phenological record of each pixel cannot be considered equally valid (White *et al*., 2002; Cook *et al*., 2005). In calculating the phenological behavior of the landscape surrounding each climate station, individual pixels within the 7×7 grid were weighted according to an index (w_{pix}) calculated as the product of four weighting factors (w), each of which ranged between 0 and 1: (a) the pixel's percent tree cover (w_{TC}), (b) the likelihood of a deciduous canopy (w_{DC}), (c) the difference in elevation between the pixel and the station (w_{VD}) and (d) the horizontal distance between the pixel and the station (w_{HD}). The data used for these calculations are displayed in Fig. 2.

The weight by tree cover (w_{TC}) (Fig. 2a) was determined from the 500 m MODIS vegetation continuous fields percentage tree cover (VCF_{TC}) product (Hansen *et al*., 2003) where:

$$w_{TC} = VCF_{TC}/100. \quad (1)$$

Weight by deciduous cover (w_{DC}) (Fig. 2b) was determined by a pixel's average canopy minimum (winter, v_{min}) and maximum (full flush, v_{max}) cover (see Fisher *et al*., 2006 for definition and calculation). An ideal deciduous canopy has a nearly flush canopy in the summer ($v_{max} = 0.8$) and is bare in the winter ($v_{min} = 0$). Therefore, deciduous cover weight was determined by Cartesian distance in v_{max} and v_{min} space:

$$w_{DC} = 1 - \sqrt{(v_{min})^2 + (v_{max} - 0.8)^2}. \quad (2)$$

Pixel topography (Fig. 2c) was determined from resampled Shuttle Radar Topography Mission (SRTM, http://seamless.usgs.gov/) data, and significant gaps

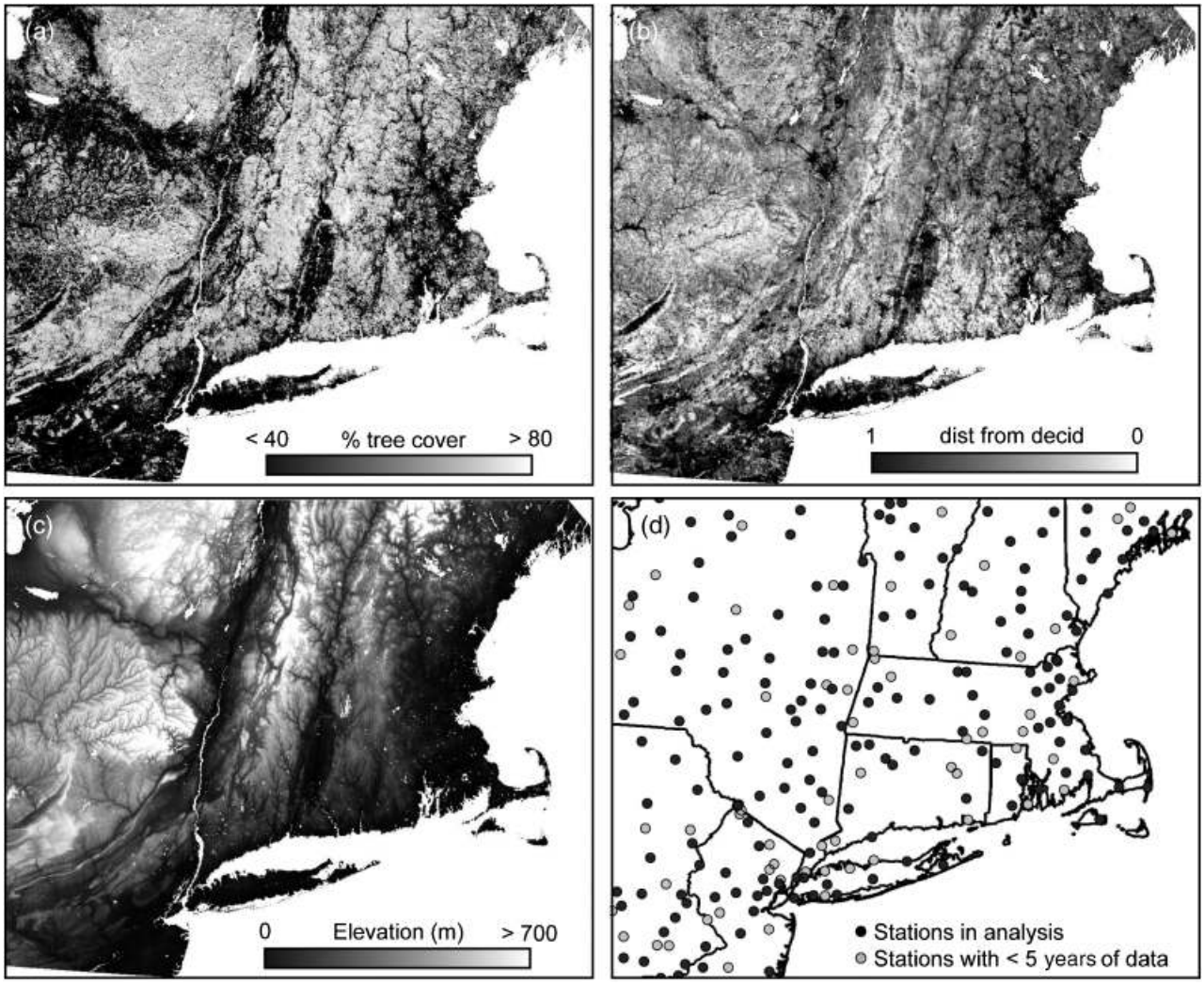

Fig. 2 Individual pixels in a 7×7 (3.5 km) grid surrounding each climate station are weighted by their estimated forest cover, estimated deciduous cover, topographic proximity to the station elevation (within 50 m), and absolute horizontal distance from the climate station. Data sets used in this calculation include: (a) percent forest cover from Moderate Resolution Imaging Spectrometer vegetation continuous fields, (b) Cartesian distance from 'perfect' deciduous behavior based on phenological minimum and maximum, (c) topography from Shuttle Radar Topography Mission and National Elevation Dataset, and (d) the station location. Stations with at least 1 year of uninterrupted temperature data from 2000 to 2005 are gray, and stations with at least 5 years of data are black (used in this analysis).

filled with National Elevation Dataset (NED) data. Weight by absolute vertical distance (w_{VD}) decreased linearly by 0.02 units m^{-1} absolute elevation difference between the pixel and station. Pixels received zero weight if the absolute elevation difference was more than 50 m.

Weight by horizontal distance (w_{HD}) decreases linearly from one (pixel containing the station) to zero with distance, reaching 0.5 at 3.5 km. Pixels over water were assigned a w_{HD} of zero. Final pixel weight was calculated as

$$w_{pix} = w_{TC} \times w_{DC} \times w_{VD} \times w_{HD}. \quad (3)$$

Vegetation cover climate-phenology model

Our analysis is based on the entire trajectory of spring green-up, as described by GV, which we model as a logistic (sigmoid) function, as shown in Eqn (4)

$$v_i = v_{min} + v_{amp}\left(\frac{1}{1 + e^{b-cx}}\right). \quad (4)$$

This functional form has been previously applied to phenological modeling (Dixon, 1976; Zhang *et al*., 2003; Beck *et al*., 2005; Fisher *et al*., 2006; Richardson *et al*., 2006) and is also commonly used in biometric models

(Sit & Poulin-Costello, 1994). Here, v_{min} and v_{amp} fit the minimum winter greenness and seasonal amplitude, respectively, the b and c parameters control the phase and steepness of the greenup curve (see Richardson *et al.*, 2006 for additional details), and x represents the driving variable. In the null model, x is the Julian day (DOY_i); in the spring warming model, x is the heat sum (HDD_i) on DOY_i.

Optimization is achieved through a weighted least squares approach, conducted using the Newton minimum distance algorithm, with weights of w_i (Fisher *et al.*, 2006). We take the point where $v_i = (v_{min} + v_{amp})/2$, or the half-maximum, as a critical value: in the null model, D_{50} is the value of DOY_i at the half-maximum, while in the spring warming model, H_{50} is the value of HDD_i at the half-maximum. Phrased differently, H_{50} is the temperature requirement at the onset of greenness (D_{50}). The critical forcing temperature (F^*) is calculated as the average temperature requirement ($\bar{H}_{50}$).

HDD is calculated as the cumulative sum temperature above T_{base} from time t_0. Standard literature values for T_{base} and t_0 are 4 °C and January 1st, respectively, but others have found that these values may be optimized for specific ecosystems (e.g. Chuine, 2000; Karlsson *et al.*, 2003). Previous studies indicate that F^* can be derived effectively at a single location, but often cannot predict the start of spring at other sites (e.g. Schaber, 2002; Richardson *et al.*, 2006). Therefore, it seems likely that F^* values may vary across space, but here we assume that the parameters T_{base} and t_0 are consistent (see 'Spatial heterogeneity of spring warming parameters (T_{base} and t_0)' for an exploration of this assumption). We used a grid search on the full data set to determine the values of T_{base} and t_0, while allowing F^* to vary. The grid search was conducted by evaluating fit RMSE at each climate station (fitting v, b, and c accordingly) with T_{base} values ranging from 1.5 to 7.5 °C in 0.5 °C increments and t_0 from 20 (January 20th) to 110 (April 19th) in 5-day increments. In each run, data points (i) in the time series which fell before t_0 ($DOY_i < t_0$) were assigned a value of $HDD_i = 0$. Best overall model fit across all climate stations as judged by weighted RMSE was achieved with $t_0 = 80$ (April 4th) and $T_{base} = 5.0$ °C (Fig. 3).

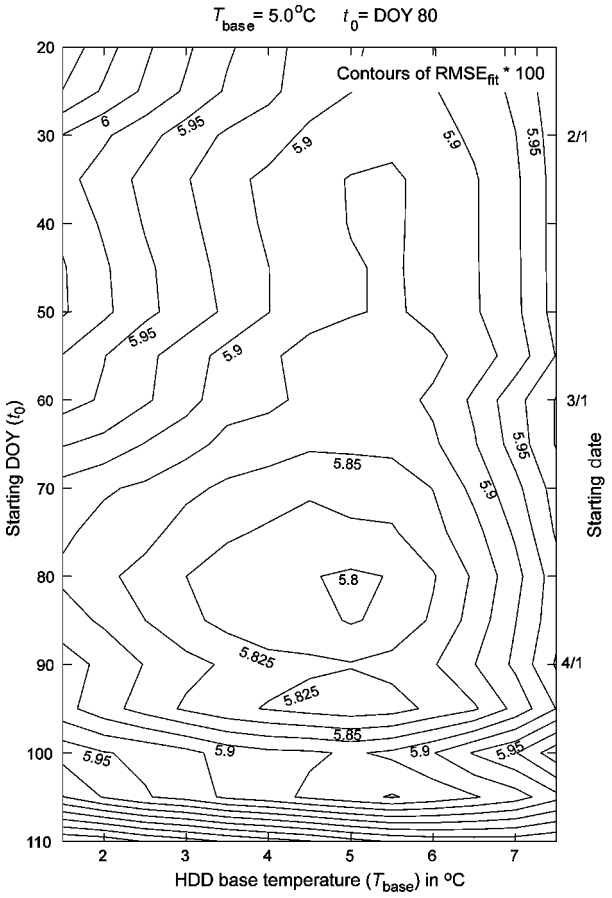

Fig. 3 Result of grid-search for best possible starting parameters. Best minimum is found at $T_{base} = 5$ °C and $t_0 = 80$ (~March 20th). Contours are in Root mean square error of spectral mixture analysis ($RMSE_{fit}$), indicating best possible fit when all data points are fit simultaneously in heating degree day (HDD) space.

Analysis of spring warming and null models

Using values of $t_0 = 80$ and $T_{base} = 5.0$ °C, D_{50} and H_{50} were determined at the 49 grid cells surrounding each station. The ability of the spring warming model (in HDD units) or null model (in DOY units) to capture interannual variability was evaluated at each grid cell by calculating the standard deviation of the residual between the actual date of onset (D_{50}) and the spring warming predicted date of onset (D'_{50}) or null model predicted date of onset ($\bar{D}_{50}$). A perfect spring warming model prediction will yield a low standard deviation between the residuals of D_{50} and D'_{50} (STD_{spring}); an interannually invariant forest (perfect null model) will produce a low standard deviation between D_{50} and $\bar{D}_{50}$ (STD_{null}). The predicted date of onset from the spring warming model (D'_{50}) is calculated as the DOY_i each year where $HDD_i = F^*$.

The standard deviation metric evaluates the ability of a given model to predict a single, prespecified state of development (D_{50} or H_{50}), but cannot assess the ability of the null or spring warming model to describe the full greenup profile (e.g. Richardson *et al.*, 2006). To accomplish this latter goal, we used a cross-validation approach (Hastie *et al.*, 2001) whereby GV_i data from a single year are tested against the predictions of a model fit using the other 5 years of data. In a perfect model, the

HDD curve (smoothed GV, or v_i) can consistently predict the shape and phase of the data points in the greenup curve (GV_i). Therefore, the fit from any selection of years should correctly predict the years not included in the analysis. This bootstrap-type method, repeated for every year, quantifies how well the mean behavior of smoothed GV (v_i) represents interannual variability in both DOY and HDD terms. We summarize the validation by calculating an average r^2 value across all years for both the null (R^2_{null}) and spring warming (R^2_{spring}) models. The r^2 for each year is calculated as in Eqn (5)

$$r^2 = 1 - \frac{SSE}{SSM} = 1 - \frac{\sum\left[(v_i - GV_i)^2 \times w_i\right]}{\sum\left[\left(v_i - \overline{GV}(w)\right)^2 \times w_i\right]}. \quad (5)$$

Here, SSE is the sum of squares of the validation error, SSM is the sum of squares of the mean, w_i is the weight at data point i from the spectral RMSE, v_i is the value at i of the sigmoid curve (fit to all years except the year in question), GV_i is green vegetation fraction at data point i (from the year in question), and $\overline{GV}(w)$ is the weighted mean of all GV_i from the year in question.

A key objective of the present research is to determine whether, across a region, HDD is a better predictor of spring phenology than DOY. The relative merit of these two approaches is quantified using what we refer to as the climate sensitivity ratio (CSR), calculated using both r^2 and standard deviation metrics [Eqn (6a,b)].

$$CSR_{STD} = \log\left(\frac{STD_{spring}}{STD_{null}}\right), \quad (6a)$$

$$CSR_{r^2} = \log\left(\frac{1 - R^2_{spring}}{1 - R^2_{null}}\right), \quad (6b)$$

In both cases, $CSR < 0$ indicates that the spring warming model captures interannual variability more effectively than the null model.

Results and discussion

Starting model parameters

Across all sites, the grid search for T_{base} and T_0 parameters (Fig. 3) resulted in a minimum model prediction error at $T_{base} = 5\,^{\circ}C$ and $t_0 = DOY\ 80$ (March 20). The base temperature is within the range found by Chuine *et al*. (1998) and Richardson *et al*. (2006) in a spring warming model, and similar to results presented by other researchers (Karlsson *et al*., 2003). The accumulation starting date is later than has been used by many researchers, but is consistent with observations that spring phenology is insensitive to mid-winter temperatures (December–February) and very sensitive to late spring temperatures (March–May; Schaber, 2002), and even in the 10 days preceding bud-break (Nizinski & Saugier, 1988).

Although there is a clear minimum, the surface has a shallow minimum trough, indicating that base temperatures ranging from 3 to 6 °C may be equally appropriate (suggesting that the model is relatively insensitive to T_{base} choice, e.g. Richardson *et al*., 2006). A wide range of starting dates (t_0) may also be valid in the aggregate, extending from February 4th (DOY ~ 35) to as late as April 4th (DOY ~ 95). This may be due to the fact that during the heart of winter, temperatures above the t_0 threshold are rarely encountered. Values of $t_0 > 90$ quickly become ill-fitting, as do T_{base} values above 6 °C, presumably because developmentally important warming events are missed with higher threshold temperatures. There are spatially coherent differences in the station-specific grid-search response surface, which suggest that there may be significant variation across sites in these phenological parameters. These differences are explored more thoroughly later in this paper. With only 6 years of data in this study, the model may not be sufficiently constrained to effectively characterize the spatial variance of T_{base} and t_0. Therefore, rather than fit separate T_{base} and t_0 parameters for each station, we focus instead on the average grid response surface across all sites (Fig. 3).

Average phenological response: $\bar{D}_{50}$ and $\bar{H}_{50}$ (F)*

There is spatial coherency in the average date of onset, $\bar{D}_{50}$ (Fig. 4a). In this study, the earliest $\bar{D}_{50}$ is in northern New Jersey, whereas the latest $\bar{D}_{50}$ is found more than a month later on the Adirondack Plateau in northern New York (NY) state (NW in the image). Late $\bar{D}_{50}$ values in the northern New Hampshire (NH) and Vermont (VT) mountains are less apparent in this study than in Fisher & Mustard (2006), but this is possibly due to a bias in station locations (more likely to occur in a valley than on mountain slopes or peaks). Other late $\bar{D}_{50}$ values appear in the Catskill Mountains of NY, and coastal Maine (ME). The late $\bar{D}_{50}$ on the southern Massachusetts (MA) coast and islands are possibly influenced by ocean proximity and sandy substrate (Motzkin *et al*., 2002).

The map of the critical forcing temperature (Fig. 4b, F^*), or mean HDD requirement to obtain 50% cover is less spatially coherent than the $\bar{D}_{50}$ map, but still retains significant spatial patterning. The most prominent feature of this map is a coastal–continental gradient overprinted on a latitudinal gradient where high F^* values are found toward the south-east, and low values to the

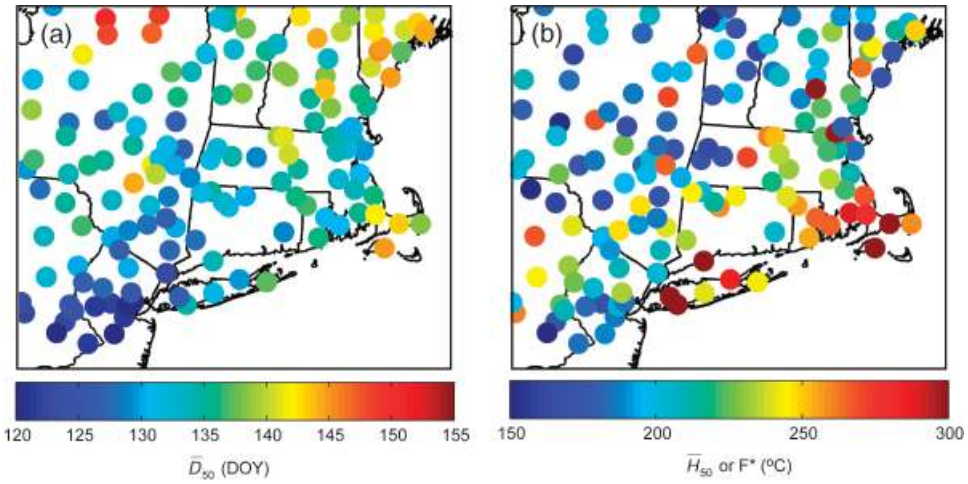

Fig. 4 Maps of the average date of onset ($\bar{D}_{50}$) (a), and the calculated critical forcing temperature (F^*), calculated as the interannual average heating degree day reached at when the canopy is at 50% cover (D_{50}).

north, similar to results presented by Jenkins *et al*., 2002. In F^*, the NY Adirondacks are similar to nearby stations, and do not appear as outliers, as in $\bar{D}_{50}$ in Fig. 4a. Gradients that were not apparent in the $\bar{D}_{50}$ map (Fig. 4a), such as coastal-inland patterns are clear in the F^* map. The wide range of best-fit F^* values (150–300 °C) implies that a single temperature forcing requirement will not successfully predict interannual greenup (D_{50}) across sites. With average New England April–May temperatures of 10 °C (NCDC, http://www.ncdc.noaa.gov/), minus the $T_{base} = 5$ °C threshold, the variance of 75 degree days becomes a prediction error of 15 days (75 degree days/5 °C day^{-1} = 15 days). Together, these maps suggest that $\bar{D}_{50}$ and F^* are unrelated across the landscape, and in fact there is no correlation ($r^2 = 0.02$).

Rötzer *et al*. (2004) notes a robust positive relationship between onset and F^* in Europe. However, the work of Rötzer assumes a starting day of January 1st, long before leaf development begins. Therefore, the accumulated sum temperatures at phenologically late regions will always be higher than early regions. The described effect would be echoed in this research as a strong correlation between $\bar{D}_{50}$ and F^*, and this is not the case. A system coupled to climate and described well by spring warming will have low spatial variance of F^* while the spatial variance of $\bar{D}_{50}$ would show climatic gradients. Instead, we appear to have a variously coupled system: there is a low range of F^* values through northern New England despite a large $\bar{D}_{50}$ range, and a wide range of F^* values through southern New England, despite relatively uniform $\bar{D}_{50}$. We are left with the as of yet unanswered question, not addressed by field studies: why does the F^* metric vary so significantly across the landscape?

Null model and spring warming half-maximum prediction (STD_{null} and STD_{spring})

We investigate the hypothesis that the spring warming model can predict interannual variability more effectively than the null model. The standard deviation of the difference between interannual D_{50} and $\bar{D}_{50}$ (STD_{null}, Fig. 5a) is compared against the standard deviation of the difference between interannual D_{50} and predicted D_{50} (D'_{50}) from the critical F^* value (STD_{spring}, Fig. 5b). The null model predicts D_{50} with a mean STD_{null} of 6.64 days, while the spring warming model predicts D'_{50} with marginally improved (but insignificant) mean STD_{spring} of 6.60 days.

STD_{null} and STD_{spring} are highly correlated ($r^2 = 0.87$), suggesting that the spring warming model increases in efficacy at sites that have relatively low interannual variability. The spatial patterns between both models are similar, with the best predictability and lowest variability in a cluster from western MA and northern CT to central NY and northern NJ (Fig. 5a and b). Variance is high in coastal MA through ME, and NH. These results suggest that although the spring warming model may capture some fraction of the interannual variability, it cannot predict interannual departures with better accuracy than the mean date of onset ($\bar{D}_{50}$).

Null model and spring warming greenup profile prediction

The spatial patterns of both R^2_{null} and R^2_{spring} are relatively spatially incoherent, and indicate a range of efficacy, predicting between 50% and 90% of GV_i interannual variance. The maps are highly correlated

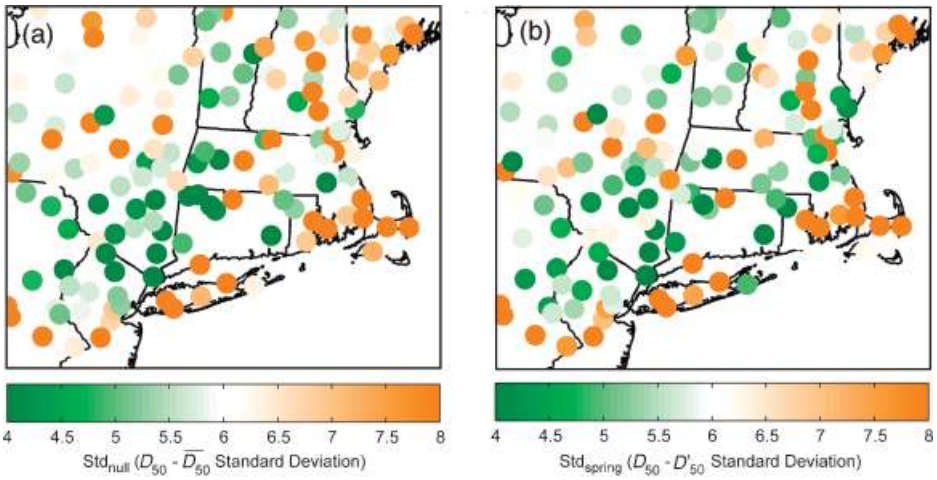

Fig. 5 Maps of STD_{null} and STD_{spring}. STD_{null} (a) is the standard deviation of the null photoperiod model, calculated as STD ($\bar{D}_{50} - D_{50}$; across all years); STD_{spring} (b) is the standard deviation of the spring warming model, or STD (D'_{50}–D_{50}). D'_{50} is predicted from the date at which heating degree day crosses the F^* value at the site. Low values in these maps suggest a well-fit model, while at higher values, the model is less effective.

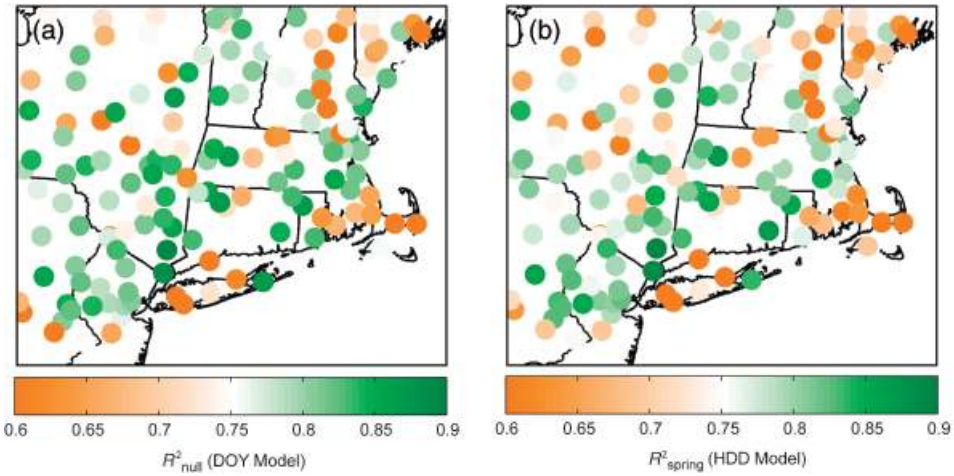

Fig. 6 Maps of prediction errors from bootstrap analysis, displayed as R^2_{null} (a) and R^2_{spring} (b). In the analysis, an average growth curve (GV_i) is calculated a combined 5 years of data and used to predict the phenology [green vegetation (GV)] of the sixth year. The goodness-of-fit (r^2) values represent the variability of this bootstrap over all 6 years (2000–2005). These values primarily tend to reflect the stability of the GV signal as perceived from the satellite rather then the efficacy of the model. However subtle differences between R^2_{null} and R^2_{spring} are more visible in the climate sensitivity ratio of Fig. 8.

($r^2 = 0.94$), and yet very different than the STD_{null} and STD_{spring} maps. We suggest that, alone, this method is sensitive to the intrinsic qualities of the data (satellite noise, cloud and snow cover) rather than the efficacy of predicting seasonal variance in DOY or HDD space.

Maps of R^2_{null} and R^2_{spring} (Fig. 6) indicate that both models fail to predict interannual variance in three distinct regions: southern coastal MA, a N–S corridor in central NH, and in upstate NY. There are two potential interpretations of these patterns: (a) satellite data in these regions cannot capture land cover and forest heterogeneity cannot be effectively fit with a sigmoid curve, or (b) neither the null model nor the spring warming model provides a reasonable basis for modeling phenology in these regions. Noise in the time-series satellite data will reduce R^2 for both models. Alternatively, at some sites, the spring warming model may fit better than the null model (e.g. Fig. 7a and b), or *vice versa* (Fig. 7c and d). In some locations, although H_{50} may be reached at a similar HDD every year, the shape of the curve could be very different, and thus yield a low r^2 value. This would indicate that although

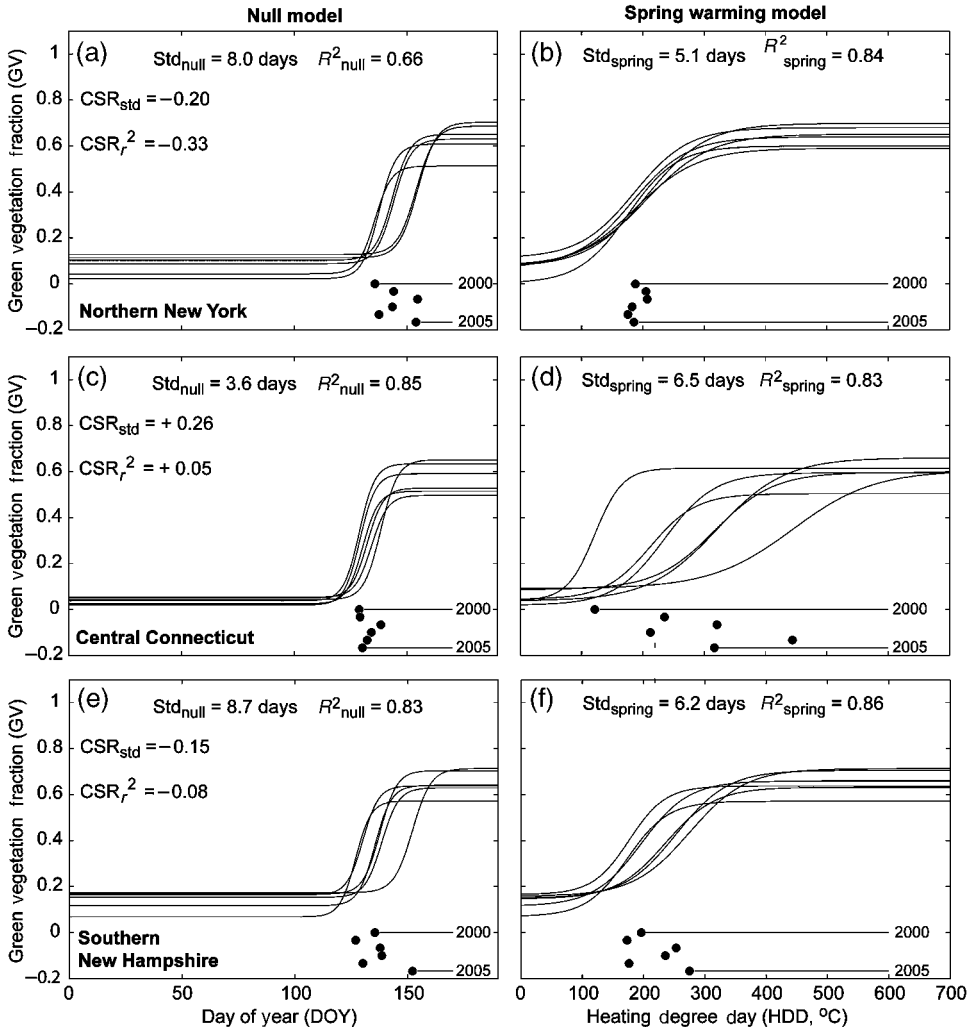

Fig. 7 Three type locality examples of greenup curves in day of year (DOY) space (a, c, e) and heating degree day (HDD) space (b, d, f), and the associated standard deviation (STD_{null} and STD_{spring}) and goodness-of-fit (R^2_{null} and R^2_{spring}) model tests. In northern New York (a and b), the spring warming model provides more interannual stability than the null model; in central CT (c and d), there is relatively little interannual variability by DOY, while modeling the same data in with a spring warming model is unstable; in southern New Hampshire (e and f) the Moderate Resolution Imaging Spectrometer pixels are both heterogeneously mixed and contain significant topographic variability, thus there is greater uncertainty in modeling interannual growth by both the null and spring warming models.

interannual H_{50} has low variance, the shape of the curve is not predictable (such as in Fig. 7e and f).

The high correlation between R^2_{null} and R^2_{spring} (Fig. 6a and b) indicate that the errors occur at each station regardless of the model used, and are, therefore, intrinsic to the station and not the model choice. We would expect that if the R^2_{null} or R^2_{spring} spatial patterns reflected the actual predictability, then the patterns of R^2_{null} and R^2_{spring} would be correlated to the maps of STD_{null} and STD_{spring}, which is only partially the case ($r^2 = 0.55$ and 0.68, respectively). These maps, taken at face value, are both difficult to interpret and appear to reflect noise or station variability more than climatological or phenological meaning.

Spatial variability and the CSR – CSR_{std} and CSR_{r2}

Both calculations of CSR have improved spatial coherency (Fig. 8) above that of the maps of $STD_{null,spring}$ and $R^2_{null,spring}$. There are generally positive values (poor spring warming predictability) in the south and negative CSR values to the north and along the NH and MA coastline. Although the gradient is not entirely clear, a species composition difference may explain the pattern of CSR in New England. In particular, the north–south gradient is suggestive of a boundary derived by Cogbill *et al*. (2002) bisecting northern hardwoods (beech and maple association) and central hardwood forests (oak and hickory association). The boundary (superimposed

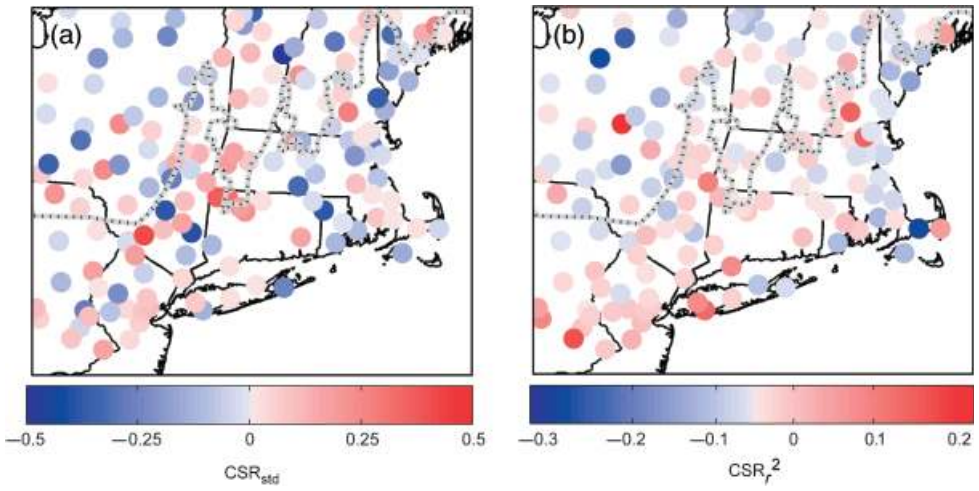

Fig. 8 Maps of the climate sensitivity ratio (CSR) reflect the ability of a sigmoid model to capture canopy cover growth in the spring warming model relative to the null model. On the left (a), CSR_{std} is the log ratio between STD_{spring} and STD_{null}, where values <0 indicate that the spring warming model is more effective than the null model (i.e. interannual variability of D_{50} is predicted by spring warming), and values >0 suggest that the spring warming model (as parameterized) is not appropriate for the site. On the right (b), CSR_{r2} is the log ratio between $(1-R^2_{spring})$ and $(1-R^2_{null})$, where values >0 imply that the spring warming model explains the greenup curve more effectively than the null model. The overlaid gray dashed line is the 'tension zone' (Cogbill *et al*., 2002), representing the approximate transition from central hardwood (oak/hickory) to northern hardwood (beech/maple) forest communities.

on Fig. 8) is derived from recorded forest composition from surveys before agricultural settlement (ca. 1623–1850). While it is important to note that recent analyses suggest significant homogenization postagriculture (Foster *et al*., 1998), the transition zone was found to be in good agreement with modern data from the US Forest Service forest inventory and analysis project (USFS FIA; mapped from Miles, 2006) data.

If the difference between the null and spring warming models shown in the CSR distribution is due to forest composition, it could imply that central hardwoods are attuned to temperature variability differently than northern hardwoods (e.g. Kramer *et al*., 2000). Alternatively, similar forests in distinctively different regions may react differently to climate (e.g. Peterson & Peterson, 2001; Richardson *et al*., 2006).

CSR_{std} is a relative of analyses in other studies, which compare interannual variability of bud-break from the null model (average day of bud-break) and various climate-phenology models (e.g. Hunter & Lechowicz, 1992; Chuine, 2000; Schaber, 2002). These analyses show that, at any given location, warming models describe interannual variability of bud-break more effectively than the annual average. However, previous observations by Richardson *et al*. (2006) demonstrated that a single set of greenup curve parameterizations in a spring warming model could not effectively explain the disparities between two deciduous forests separated by 150 km. The disparity argues strongly against the use of uniform phenology model parameters, an objective of many climate-phenology models. While the results of this study cannot support the efficacy of a uniform parameter spring warming model in interpreting temperate satellite phenologies, they do suggest operationally different mechanisms in different forest types.

Spatial heterogeneity of spring warming parameters (T_{base} and t_0)

It may be instructive to examine at least one of the underlying assumptions in the spring warming model to explain observed variance. In particular, the uniformity of the base temperature (T_{base}) and starting date of accumulation (t_0) may be an inappropriate simplification. The choice of separate T_{base} and t_0 parameters for each station would provide poor constraints for the model, as there would be six parameters (T_{base}, t_0, v_{min}, v_{max}, b, and c) used to fit 6 years of data (2000–2005). However, the observation that forest type may be a significant factor in determining phenological response to climatic variability allows an *ex post facto* exploration of T_{base} and t_0. The initial parameter grid search (described in 'Vegetation cover climate-phenology model') was performed again, but in two populations divided along the Cogbill *et al*. (2002) forest composition transition (the center line of a broad 'tension zone').

The result is displayed in two contour plots in Fig. 9, displaying the best parameter fit error minima for northern and central hardwoods. Although the populations appear to have distinct minima (separated pri-

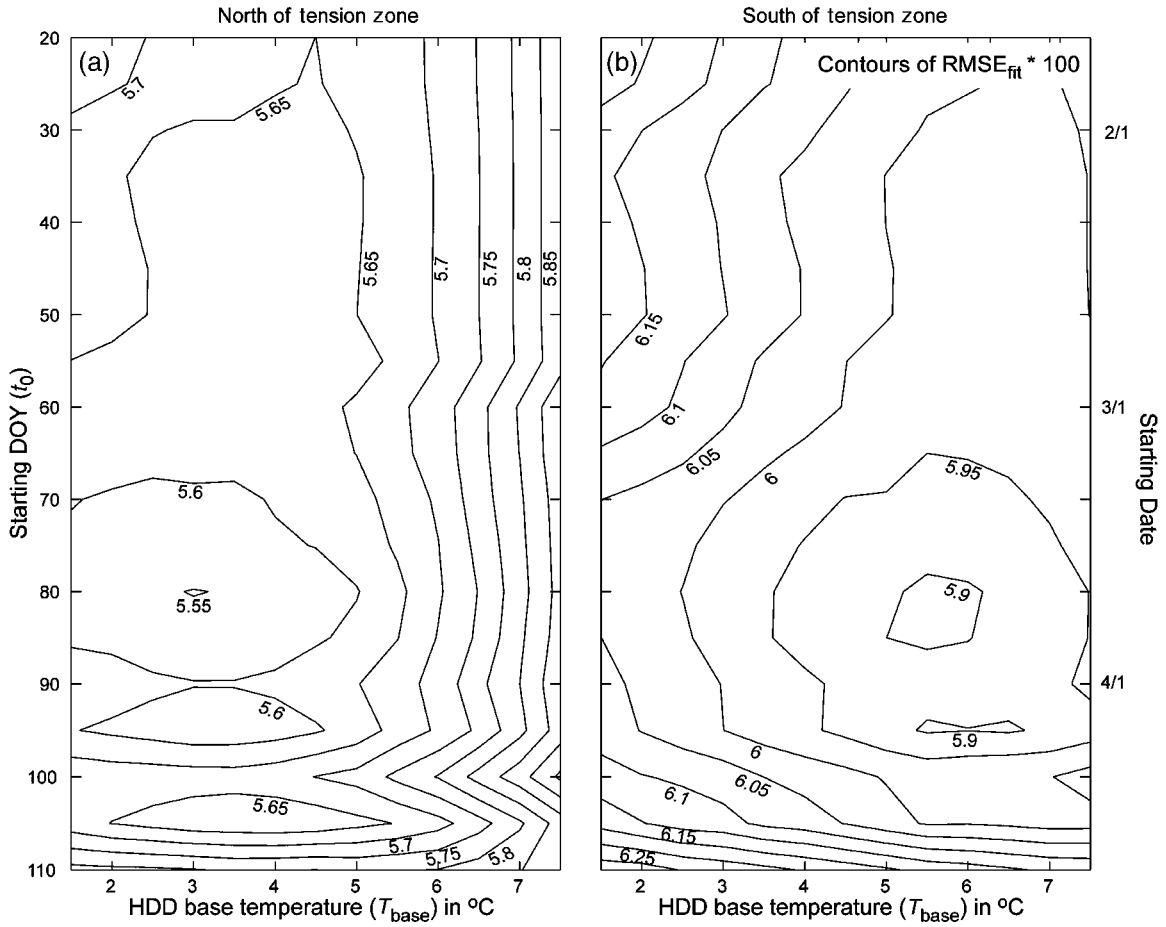

Fig. 9 Recalculated grid-search results for best starting parameters for forests north (a) and south (b) of the forest transition 'tension zone' (similar layout to Fig. 3). Both contour graphs indicate a poor specificity for $t_0 = 80$ (~March 20th), but strong trends for distinctly separate base temperatures (T_{base}). Forests north of the tension zone (a) are best modeled with $T_{base} = 3.0\,^{\circ}C$ while forests south of the tension zone (b) require higher base temperatures near 6.0 °C to begin spring growth.

marily by the best base temperature, T_{base}), the separation is insignificant. The 95% confidence interval from a $\delta\chi^2$ test (Press *et al.*, 1992) indicates that the error bounds between the north and south populations are highly overlapping (upper bound RMSE contour in the north = 0.0592, $n = 1697$; upper bound RMSE contour in the south = 0.0610, $n = 3757$). While the broad error bounds suggest a relatively low sensitivity to exact T_{base} and D_0 values in this analysis, a significant separation would imply a mechanistic difference between northern hardwood forests responding to lower temperatures than central hardwoods.

Climate-phenology model hypotheses

In this study, we observe significant differences in the climate-phenology relationship across the landscape. If we revisit the original hypotheses, it is clear that the null model (Hypothesis A) cannot account for satellite interannual variability, which has been observed to track climate in multiple studies (White *et al.*, 1997; Cook *et al.*, 2005; Fisher & Mustard, 2006). However, the oft-proposed Hypothesis B, that greenup is governed by a uniform critical forcing temperature (F^*), is also shown not to be the case in this study: the spatial variability of temperature requirements across the region (Fig. 4b) rule out this explanation. Hypothesis C, that greenup is predictable by F^* values which are consistent at any given location, is more likely; however in this study we show that large areas of southern New England are not predictable based on station-specific F^* values. From the results of this study, Hypothesis D is the only hypothesis which cannot be ruled out: greenup appears to be differentially governed by DOY or spring warming (consistent with Peterson & Peterson, 2001). However, in showing that T_{base} and t_0 parameters may also vary by location, a modified form of hypothesis C

becomes feasible: greenup is predictable by station-specific F^* values when other functional parameters (T_{base} and t_0) are stratified by forest type.

We submit that the spring warming model, despite its simplicity, may not be adequate to explain the variability seen in temperate deciduous forests. We suggest that, contrary to recent assertions, interannual phenological variability from satellite data may not be readily interpreted in climate terms (e.g. Jenkins *et al*., 2002; Schwartz *et al*., 2002), nor would we expect that climate-phenology models applied to temperature data will accurately predict large spatial scale interannual variability (e.g. Schwartz *et al*., 2006). Additional refinement and a better understanding of phenological triggers may be required before we understand the climate implications of studies which satellite phenology (Myneni *et al*., 1997; Goetz *et al*., 2005).

Conclusion

Phenological research over the last two decades has progressed in two completely independent veins: climate-phenology models derived from ground observations, and monitoring methods constructed from satellite observations. These intrinsically different lines of study are poorly linked (Schwartz & Reed, 1999; Badeck *et al*., 2004). The satellite phenology community has made the implicit assumption that interannual and average phenological observations are expressions of climatological variability (e.g. Jenkins *et al*., 2002; Zhang *et al*., 2004). This assumption is buffered by the typically large spatial extent of satellite studies: by examining regional to global patterns of variability, satellite phenological studies will detect significant spatial variability which is certainly climatological in nature (e.g. Jenkins *et al*., 2002; Schwartz *et al*., 2002; Zhang *et al*., 2004). However, the robustness of these studies at large global scales does not necessarily translate to accurate or precise records of phenological variability on the ground (Schwartz *et al*., 2002).

While, in phenological work, the satellite community has historically been compelled to assume regional or landscape-scale homogeneity (usually for lack of information otherwise; Schwartz & Reed, 1999; Jenkins *et al*., 2002; Zhang *et al*., 2003 but see, Bunn *et al*., 2005), ground-based phenology models have long recognized significant differences between species in reacting to climate (Lechowicz, 1984; Schaber, 2002). Conversely, the assumption common to most ground-based phenological studies is that forests of similar type in different locations respond similarly to climate variability, a supposition refuted by many phenological studies (e.g. Karlsson *et al*., 2003; Richardson *et al*., 2006), including this research.

There is great potential at the interface between satellite and ground-based phenology studies. While we found that the spring warming model did not generally hold over our study region, we set a framework for linking satellite data with simple field models using observed meteorological data. There is a great deal of potential for generating improved models of phenology from climate data which operate effectively over time and space, and can predict variability in the satellite record.

Acknowledgements

The Landsat database was obtained under grants from the University of Rhode Island/NOAA Cooperative Marine and Education Research Program, the National Oceanographic Partnership Program, NASA Land Use and Land Cover Change, and the Rhode Island Department of Environmental Management. Climate data were provided by the National Oceanographic and Atmospheric Administration (NOAA) National Climate Data Center (NCDC). Topography data (NED and SRTM) was provided by the United Stated Geological Survey (USGS). Forest cover map curtsey of the Global Land Cover Facility (GLCF) at the University of Maryland, College Park. The research was partially supported by a grant from the National Estuarine Research Reserve. We are grateful for feedback from Matthew Vadeboncoeur, Ruth DeFries, and two anonymous reviewers, as well as data from Charles Cogbill and Elizabeth LaPoint at the USDA Forest Service.

References

Adams JB, Smith MO, Gillespie AR (1993) Imaging Spectroscopy: Interpretation Based on Spectral Mixture Analysis. In: *Remote Geochemical Analysis: Elemental and Mineralogical Composition* (eds Pieters CM, Englert PAJ), pp. 145–166. Press Syndicate of University of Cambridge, Cambridge, UK.

Anyamba A, Tucker CJ, Mahoney R (2002) From El Niño to La Niña: vegetation response patterns over East and Southern Africa during the 1997–2000 Period. *Journal of Climate*, **15**, 3096–3103.

Badeck FW, Bondeau A, Böttcher K *et al*. (2004) Responses of spring phenology to climate change. *New Phytologist*, **162**, 295–309.

Beck PSA, Atzberger C, Høgda KA *et al*. (2005) Improved monitoring of vegetation dynamics at very high latitudes: a new method using MODIS NDVI. *Remote Sensing of Environment*, **100**, 321–334.

Bradley BA, Jacob RW, Hermance JF *et al*. (2006) A curve fitting procedure to derive inter-annual phenologies from time series of noisy satellite NDVI data. *Remote Sensing of Environment*, doi: 10.1016/j.rse.2006.08.002.

Bunn AG, Goetz SJ, Fiske GJ (2005) Observed and predicted responses of plant growth to climate across Canada. *Geophysical Research Letters*, **32**, L16710.

Cannell MGR, Smith RI (1983) Thermal time, chill days, and prediction of budburst in *Picea sitchensis*. *Journal of Applied Ecology*, **20**, 951–963.

Cesaraccio C, Spano D, Snyder RL *et al*. (2004) Chilling and forcing model to predict bud-burst of crop and forest species. *Agricultural and Forest Meteorology*, **126**, 1–13.

Chuine I (2000) A unified model for budburst of trees. *Journal of Theoretical Biology*, **207**, 337–347.

Chuine I, Cour P, Rousseau DD (1998) Selecting models to predict the timing of flowering of temperate trees: implications for tree phenology modeling. *Plant, Cell and Environment*, **22**, 1–13.

Chuine I, Yiou P, Viovy N *et al*. (2004) Grape ripening as a past climate indicator. *Nature*, **432**, 289–290.

Cogbill CV, Burk J, Motzkin G (2002) The forests of presettlement New England, USA: spatial and compositional patterns based on town proprietor surveys. *Journal of Biogeography*, **29**, 1279–1304.

Cook BI, Smith TM, Mann ME (2005) The North Atlantic Oscillation and regional phenology prediction over Europe. *Global Change Biology*, **11**, 919–926.

Dixon KR (1976) Analysis of seasonal leaf fall in north temperate deciduous forests. *Oikos*, **27**, 300.

Fisher JI, Mustard JF (2006) Interannual phenological variability from MODIS data: from fine to coarse satellite scales. *Remote Sensing of Environment*, in press.

Fisher JI, Mustard JF, Vadeboncoeur MA (2006) Green leaf phenology at Landsat resolution: scaling from the field to the satellite. *Remote Sensing of Environment*, **100**, 265–279.

Fitter AH, Fitter RSR (2002) Rapid changes in flower time in British plants. *Science*, **296**, 1689–1691.

Foster DR, Motzkin G, Slater B (1998) Land-use history as long-term broad-scale disturbance: regional forest dynamics in Central New England. *Ecosystems*, **1**, 96–119.

Goetz SJ, Bunn AG, Fiske GJ *et al*. (2005) Satellite-observed photosynthetic trends across boreal North America associated with climate and fire disturbance. *Proceedings of the National Academies of Science*, **102**, 13521–13535.

Hanninen H (1995) Effects of climatic change on trees from cool and temperate regions: an ecophysiological approach to modeling of bud burst phenology. *Canadian Journal of Botany*, **73**, 183–199.

Hansen MC, DeFries RS *et al*. (2003) *500m MODIS Vegetation Continuous Fields*. The Global Land Cover Facility, College Park, MD.

Hastie T, Tibshirani R, Friedman J (2001) *The Elements of Statistical Learning: Data Mining, Inference, and Prediction*. Springer, New York.

Hunter AF, Lechowicz MJ (1992) Predicting the timing of budburst in temperate trees. *Journal of Applied Ecology*, **29**, 597–604.

Jenkins JP, Braswell BH, Frolking SE *et al*. (2002) Detecting and predicting spatial and interannual patterns of temperate forest springtime phenology in the eastern US. *Geophysical Research Letters*, **29**, 54.

Karlsson PS, Bylund H, Neuvonen S *et al*. (2003) Climatic response of budburst in the mountain birch at two areas in northern Fennoscandia and possible responses to global change. *Ecography*, **26**, 617–625.

Kramer K, Leinonen I, Loustau D (2000) The importance of phenology for the evaluation of impact of climate change on growth of boreal, temperate and Mediterranean forest ecosystems: an overview. *International Journal of Biometeorology*, **44**, 67–75.

Lechowicz MJ (1984) Why do temperate deciduous trees leaf out at different times? Adaptation and ecology of forest communities. *American Naturalist*, **124**, 821–842.

Lotsch A, Friedl MA, Anderson BT *et al*. (2005) Response of terrestrial ecosystems to recent northern hemispheric drought. *Geophysical Research Letters*, **32**, L06705, doi: 10.1029/2004GL022043.

Miles PD (2006) *Forest Inventory Mapmaker Web-Application Version 2.1*. US Department of Agriculture, Forest Service, North Central Research Station, St. Paul, MN. Available online at: www.ncrs2.fs.fed.us/4801/fiadb/index.htm

Motzkin G, Ciccarello SC, Foster DR (2002) Frost pockets on a level sand plain: does variaition in microclimate help maintain persistent vegetation patterns? *Journal of the Torrey Botanical Society*, **129**, 154–163.

Myneni R, Keeling CD, Tucker CJ *et al*. (1997) Increased plant growth in the northern high latitudes from 1981 to 1991. *Nature*, **386**, 698–702.

Nizinski JJ, Saugier B (1988) A model of leaf budding and development for a mature *Quercus* forest. *Journal of Applied Ecology*, **25**, 643–652.

Peñuelas J, Filella I, Comas P (2002) Changed plant and animal life cycles from 1952 to 2000 in the Mediterranean region. *Global Change Biology*, **8**, 531–544.

Peterson DW, Peterson DL (2001) Mountain hemlock growth responds to climatic variability at annual and decadal time scales. *Ecology*, **82**, 3330–3345.

Potter C, Klooster S, Myneni R *et al*. (2003) Continental-scale comparisons of terrestrial carbon sinks estimated from satellite data and ecosystem modeling 1982–1998. *Global and Planetary Change*, **39**, 201–213.

Press WH, Teukolsky SA, Vetterling WT *et al*. (1992) *Numerical Recipes in C: The Art of Scientific Computing*, 2nd edn. Cambridge University Press, Cambridge.

Rötzer T, Grote R, Pretzsch H (2004) The timing of bud burst and its effect on tree growth. *International Journal of Biometeorology*, **48**, 109–118.

Rathcke B, Lacey EP (1985) Phenological patterns of terrestrial plants. *Annual Review of Ecology and Systematics*, **16**, 179–214.

Richardson AD, Bailey AS, Denny EG *et al*. (2006) Phenology of a northern hardwood forest canopy. *Global Change Biology*, **12**, 1174–1188.

Schaber J (2002) *Phenology in Germany in the 20th Century: Methods, Analyses, and Models*. Dissertation. University of Potsdam, Germany. April, 2002.

Schaber J, Badeck FW (2003) Physiology-based phenology models for forest tree species in Germany. *International Journal of Biometeorology*, **47**, 193–201.

Scheifinger H, Menzel A, Koch E *et al*. (2002) Atmospheric mechanisms governing the spatial and temporal variability of phenological phases in central Europe. *International Journal of Climatology*, **22**, 1739–1755.

Schwartz MD, Ahas R, Aasa A (2006) Onset of spring starting earlier across the Northern Hemisphere. *Global Change Biology*, **12**, 343–351.

Schwartz MD, Reed BC (1999) Surface phenology and satellite sensor-derived onset of greenness: an initial comparison. *International Journal of Remote Sensing*, **20**, 3451–3457.

Schwartz MD, Reed BC, White MA (2002) Assessing satellite-derived start-of-season measures in the coterminous USA. *International Journal of Climatology*, **22**, 1793–1805.

Sit V, Poulin-Costello M (1994) *Catalog of curves for curve fitting, Biometrics Information Handbook Series, No. 4*, British Columbia Ministry of Forests, Victoria, BC.

White MA, Nemani RR (2003) Canopy duration has little influence on annual carbon storage in the deciduous broad leaf forest. *Global Change Biology*, **9**, 967–972.

White MA, Nemani RR, Thornton PE *et al*. (2002) Satellite evidence of phenological differences between urbanized and rural areas of the Eastern United States Deciduous Broadleaf Forest. *Ecosystems*, **5**, 260–277.

White MA, Thornton PE, Running SW (1997) A continental phenology model for monitoring vegetation responses to interannual climatic variability. *Global Biogeochemical Cycles*, **11**, 217–234.

Zhang X, Friedl MA, Schaaf CB *et al*. (2003) Monitoring vegetation phenology using MODIS. *Remote Sensing of Environment*, **84**, 471–475.

Zhang X, Friedl MA, Schaaf CB *et al*. (2004) The footprint of urban climates on vegetation phenology. *Geophysical Research Letters*, **31**, L12209.

Appendix

$\mathrm{CSR}_{\mathrm{std}}$ = efficacy of spring warming model compared with null model (standard deviation)
CSR_{r^2} = efficacy of spring warming model compared with null model (r^2-test)
D_{50} = date of onset, or date at which phenology obtains half-maximum spring greenness
$\bar{D}_{50}$ = average date of onset (averaged over all years)
D'_{50} = predicted date of onset from date at which HDD obtains value F^*
DOY = day of year (1–365)
DOY_i = day of year at i
F^* = forcing requirement to obtain half maximum greenness (set equal to $\bar{H}_{50}$)
GV_i = green vegetation fraction from spectral mixture analysis at i
$\overline{\mathrm{GV}}(w)$ = weighted mean of all GV_i in a time series
H_{50} = heating degree day at half-maximum greenness
$\bar{H}_{50}$ = average heating degree day at half-maximum greenness
HDD = heating degree day (accumulated temperature sum) in spring warming model
HDD_i = heating degree day at i
i = time or temperature increment
R^2_{null} = goodness of fit of the null model in predicting full phenology curve
R^2_{spring} = goodness of fit of the spring warming model in predicting full phenology curve
RMSE_i = root mean square error of spectral mixture analysis at i
SSE = sum of squares of phenology curve error (compares GV_i against curve fit)
SSM = sum of squares of the mean (compares $\overline{GV}(w)$ against curve fit)
$\mathrm{STD}_{\mathrm{null}}$ = standard deviation of half-maximum prediction for null model
$\mathrm{STD}_{\mathrm{spring}}$ = standard deviation of half-maximum prediction in spring warming model
t_0 = starting day for accumulating heat sums in spring warming model
T_{base} = base temperature for spring warming model
T_{max} = daily maximum temperature at climate station
T_{min} = daily minimum temperature at climate station
w_{DC} = weight fraction of pixel from deciduous cover estimate
w_{HD} = weight fraction of pixel from horizontal distance
w_i = weight of data point (i) in phenology curve-fit ($w_i = \mathrm{RMSE}_i^{-1}$)
w_{pix} = weight of individual pixel surrounding climate station (0–1)
w_{TC} = weight fraction of pixel from tree cover estimate
w_{VD} = weight fraction of pixel from vertical distance
v_{amp} = phenological curve amplitude
v_{min} = phenological curve minimum
b, c = Phenological fit parameters
$\mathrm{VCF}_{\mathrm{TC}}$ = vegetation continuous fields product of tree cover